Journal of the Korean Physical Society, Vol. 56, No. 1, January 2010, pp. 462∼466

Impedance Analysis and Low-Frequency Dispersion Behavior of $Bi_4Ti_3O_{12}$ Glass

C. H. Song, M. Kim, S. M. Lee, H. W. Choi and Y. S. Yang*

Department of Nano Fusion Technology, Research Center for Dielectric and Advanced Matter Physics, Pusan National University, Busan 609-735

(Received 17 March 2009, in final form 17 June 2009)

We have studied the frequency- and the temperature-dependent dielectric relaxation for the $Bi_4Ti_3O_{12}$ glass. The frequency dependence of the electrical data has been analyzed in the frameworks of the impedance Cole-Cole formalism and the universal power law. We have found that the frequency-dependent dielectric properties exhibit low-frequency dispersion and that the relaxation behavior is far from a Debye-type behavior. The similar values of the ac and the dc activation energies of the electrical conduction from two different models, the complex impedance formula and the power law, indicate that the activation energy is an appropriate parameter for explaining the electrical relaxation and conduction mechanisms. The frequency-dependent conductivities overlap on a single master curve, irrespective of temperature, in the glass region, implying the existence of a universal ionic relaxation process in this glass system.

PACS numbers: 72.80.Ng, 72.20.Ee, 77.22.Gm
Keywords: Glass, Low-frequency dispersion, Activation energy, Master curve
DOI: 10.3938/jkps.56.462

I. INTRODUCTION

Recently, lead has been expelled from many commercial applications and materials owing to concerns regarding its toxicity. For this reason, much interest has been shown toward research on lead-free materials that have a large dielectric constant and ferroelectricity.

Bismuth titanate, $Bi_4Ti_3O_{12}$ (BIT), is one of the most studied material among the bismuth layered ferroelectrics $SrBi_2Ta_2O_9$ and $SrBiNb_2O_{12}$ because of its excellent ferroelectric properties and lead-free nature. Generally, the bismuth layered structure can be represented by the general formula $(Bi_2O_2)^{2+}$ $(A_{m-1}B_mO_{3m+1})^{2-}$, where A is an alkali or an alkaline earth ion and B is a transition metal ion such as Ti or Nb. For BIT, A = Bi, B = Ti, and m = 3. Namely, BIT has triple layers of TiO_6 octahedral layers with Bi between $(Bi_2O_2)^{2+}$. BIT is monoclinic with the space group B1a1 at room temperature and tetragonal with I4/mmm symmetry in the paraelectric state at temperatures above the Curie temperature. It has a high Curie temperature (T_c = 948 K) and a large spontaneous polarization ($P_s = \sim 50$ $\mu C/cm^2$) with useful properties that can be applied for optical memories and for high-temperature piezoelectric and electro-optic devices [1–5]. Nowadays, glass and glass-ceramics, especially the dielectric relaxation and electrical conduction mechanism of those materials, are an increasing field of research in view of science and technology. It is advantageous to be able to fabricate BIT glass without a glass former. The dielectric, optical, and structural properties, as well as the crystallization process from glass, have been reported [6–8], but there has been a lack of systematic study on the temperature- and the frequency-dependent dielectric properties for BIT glass.

The aim of this study is to investigate the dielectric relaxation and the electrical conduction mechanisms of $Bi_4Ti_3O_{12}$ glass. The experimental data have been analyzed using the complex impedance Cole-Cole formalism and the Jonscher's power law.

II. EXPERIMENT

To fabricate the $Bi_4Ti_3O_{12}$ crystalline powder, Bi_2O_3 and TiO_2 were well mixed in a 2.4 : 3 mole ratio (20% excess Bi_2O_3) and were synthesized for 6 hours at 873 K. It was ground and synthesized for 12 hours at 1073 K. The synthesized powder was confirmed to have a monoclinic $Bi_4Ti_3O_{12}$ structure at room temperature from X-ray diffraction (XRD) patterns. This powder was then melted in a platinum tube in an electric furnace at 1473 K. The melt was quenched by using a twin-roller to form a glass state. The obtained glass sample was ~ 25 μm thick with a light-yellow color and was transparent.

XRD and differential thermal analysis (DTA) measurements were performed to insure the sample was glass

---

*E-mail: ysyang@pusan.ac.kr; Fax: +82-55-350-5837

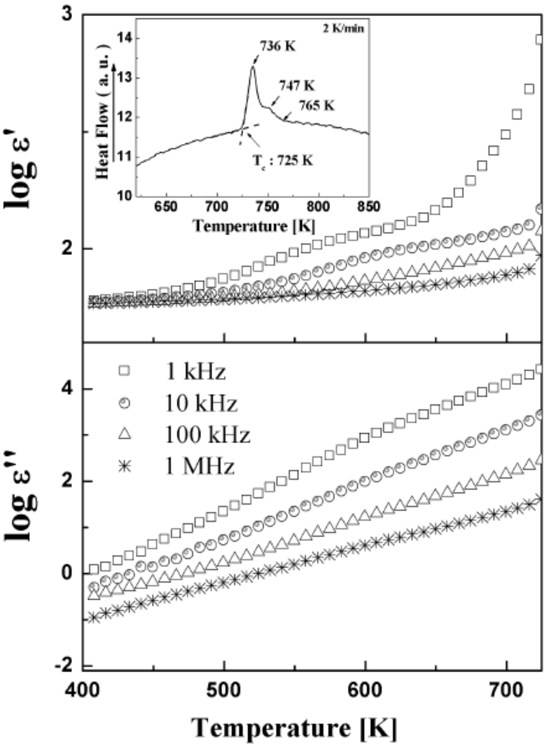

Fig. 1. Temperature dependence of the dielectric constant for $Bi_4Ti_3O_{12}$ glass. The inset is the DTA curve and is given as a reference to show the crystallization temperature, T_c = 725 K, and the exothermic behavior.

and to check the thermal and the structural behaviors during the phase transition from glass to crystal phases. The dielectric property of $Bi_4Ti_3O_{12}$ glass was measured by using an impedance/gain-phase analyzer. Circular golden electrodes of 2.25 mm^2 were put on both sides of the sample, and gold leads were attached to them with gold paste. The frequency was varied from 100 Hz to 15 MHz, and the highest temperature reached was 725 K at a heating rate of 2 K/min.

III. RESULT AND DISCUSSION

Figure 1 shows the temperature dependence of the real (ε') and the imaginary (ε'') parts of the dielectric constant for $Bi_4Ti_3O_{12}$ glass. A linear-log scale is used to present a clear view at a low value of the dielectric constant. It is recognized, from the DTA curve in the inset of the figure that the crystallization temperature (T_c) is 725 K. Our investigation of the dielectric properties in this research is restricted to temperatures below T_c, *i.e.*, to the glass region. As can be seen in Fig. 1, both ε' and ε'' increase with increasing temperature, which is caused by the activated movement of ionic charge carriers. Interestingly, the rates of increase of ε'' with frequency and temperature are close each other. However, the difference in ε' values at a given temperature are more pronounced with decreasing frequencies from 1 MHz to 1 kHz, which indicates that the relaxation dispersion of the dielectric polarization at low frequency is pronounced in the glass region. A further explanation of this phenomenon is given in Fig. 2.

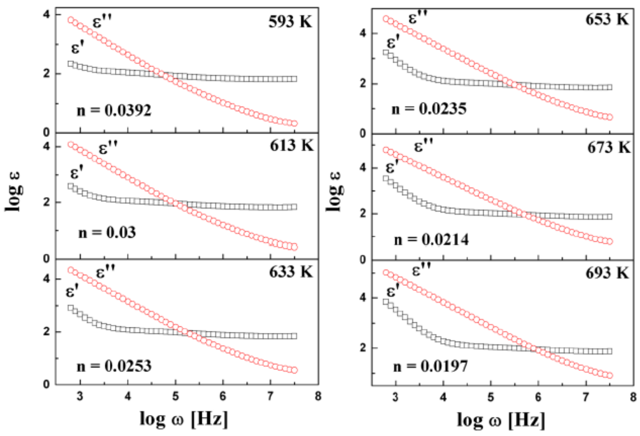

Fig. 2. (Color online) Frequency dependence of the real and the imaginary parts of the dielectric constant on a log-log scale at various temperatures for $Bi_4Ti_3O_{12}$ glass. The figure shows a typical low-frequency dispersion (LFD) relationship.

Figure 2 shows the frequency dependence of the dielectric constants ε' and ε'' on a log-log scale at various temperatures in the glass region. The ε' has a strong dispersion below some frequency; meanwhile ε'', which is dominated by the conduction of mobile charge, keeps the shape of a single slope. This behavior becomes stronger with increasing temperature and is known as low-frequency dispersion (LFD). LFD has been intensively studied by Jonscher and is understood in that the conducting process is due to ion hopping and to slowly mobile charge carriers and can be written as [9]

$$\varepsilon(\omega) \propto (i\omega)^{n-1} \propto \left(\sin\frac{n\pi}{2} - i\cos\frac{n\pi}{2}\right)\omega^{n-1}, \tag{1}$$

$$\frac{\varepsilon''(\omega)}{\varepsilon'(\omega)} = \cot\frac{n\pi}{2}, \tag{2}$$

where ε and ω are the complex dielectric constant and the frequency, respectively. In Eq. (2), for a fixed value of n, the ratio of ε'' to ε' is constant, and the shapes of ε' and ε'' as functions of frequency are the same (parallel) with a constant offset on a log-log scale. In Fig. 2, as an example, below log $\omega \sim 3.5$ at 633 K, the parallel behavior between ε' and ε'' can be well recognized. However, the parallelism between ε' and ε'' deviates, and the value of n decreases with increasing temperature. In Fig. 2, n decreases, and the rate of ε' (the slope of ε') increases at low frequency with increasing temperature. Thus, the rate of increase of ε'' is higher than that of ε', which also explains the electrical conductivity and the increased tan loss for a fixed frequency with increasing temperature.

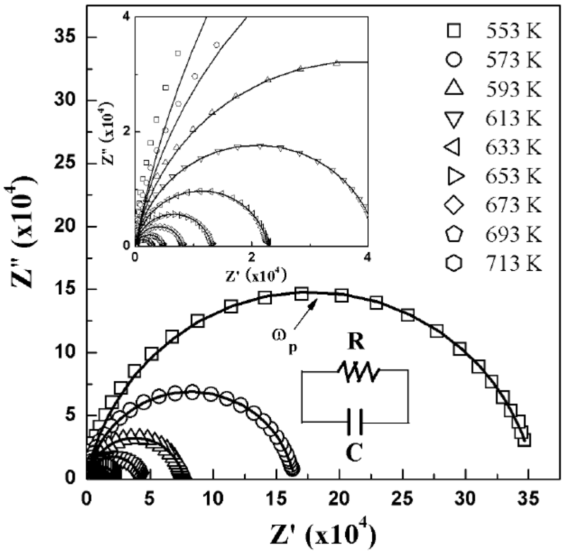

Fig. 3. Frequency dependence of the complex impedance Cole-Cole plot and an equivalent circuit for $Bi_4Ti_3O_{12}$ glass. Symbols are the experimental data, and solid lines are the results of the fit from the Cole-Cole impedance formalism of Eq. (3). The inset is a magnification of the Cole-Cole plot for the low impedance region.

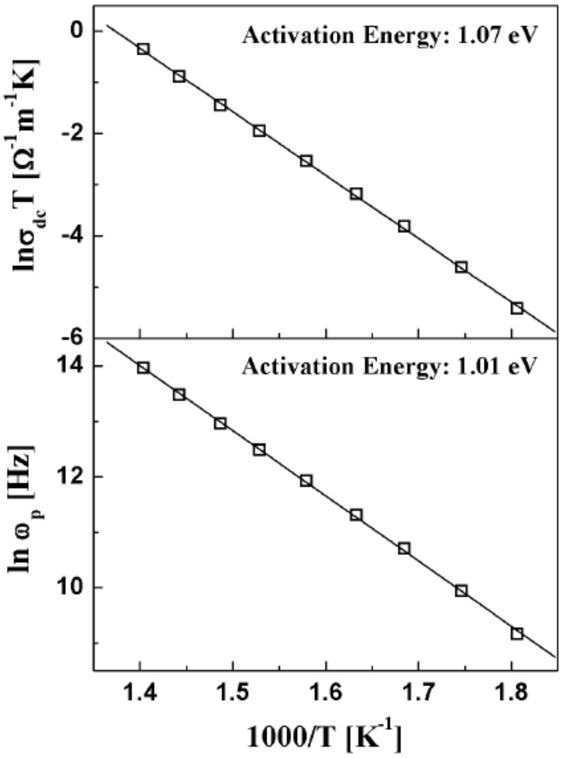

Fig. 4. Arrhenius plot to obtain the dc and the ac activation energies of the conductivity for $Bi_4Ti_3O_{12}$ glass by using the impedance Cole-Cole formula. σ_{dc} (=1/Z_o) and ω_p are obtained from a fit of Eq. (3). The solid lines represent the best fits with the Arrhenius relations.

Figure 3 represents the complex impedance Cole-Cole plot to investigate the electric transport mechanism in the glass region. The inset is simply a magnification of the complex impedance Cole-Cole plot in the temperature range from 633 K to 713 K for a clear view. Dielectric relaxation measurements are usually performed in the frequency domain, and the data can be represented on the complex impedance plane by using the Col-Cole function. The impedance representation can also be obtained from a model equivalent electrical circuit with resistance R and capacitance C, as shown in Fig. 3. The impedance function corresponding to the circuit in the figure can be written by using the Cole-Cole formalism [10]

$$Z^* = \frac{R}{[1 + (\imath\omega\tau)^\alpha]}, \tag{3}$$

where $\tau = RC$ and the exponent α characterizes a weight on the distribution of the relaxation time with $0 \leq \alpha \leq 1$. The system has a Debye behavior in the case of $\alpha = 1$. For the $Bi_4Ti_3O_{12}$ glass in this study, α varies from 0.89 to 0.9 in the temperature range from 573 K to 713 K. This represents the fact that the system is a non-Debye type systems and the behavior is known to originate from ionic conduction of hopping among moderately random free-energy barriers with a broad distribution of relaxation times [11]. In Fig. 3, the points are the experimental data, and the lines are fits to Eq. (3). The dc resistivity (Z_o or R) is determined as the impedance value at which the extrapolated line from the circle intercepts the real axis as $\omega \to 0$. The drastic decrease of Z_o as temperature increases is understood to be due to thermal agitation and to the increased hopping rates of conducting ions.

Figure 4 is an Arrhenius plot to calculate the dc and the ac activation energies. In using the Arrhenius equation, we assumed that charge carriers were thermally activated and that the ac and the dc conductivities changed monotonically with temperature. The dc conductivity ($1/Z_o$) and ω_p, the frequency at the maximum value of Z'' in Fig. 3, with the corresponding dc and ac activation energies (E_{dc} and E_{ac}) can be written as follows [12–14]:

$$\sigma_{dc}T = \sigma_o \exp(-E_{dc}/k_BT), \tag{4}$$

$$\omega_p = \omega_o \exp(-E_{ac}/k_BT). \tag{5}$$

The activation energies of the dc and the ac conduction calculated from the straight lines in Fig. 4 by using Eqs. (4) and (5) are 1.07 eV and 1.02 eV, respectively. The similar values of the dc and the ac activation energies for electrical conduction show that the heights of the random energy barriers for short and long distance movements of charge carriers are not so different from each other.

Figure 5 shows the frequency dependence of the real conductivity $\sigma(\omega)$ for various temperatures. The solid

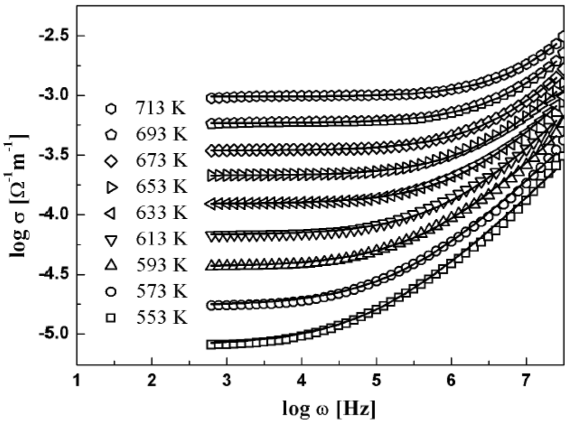

Fig. 5. Frequency dependence of the real conductivity $\sigma(\omega)$ for $Bi_4Ti_3O_{12}$ glass at several temperatures. Symbols are data, and lines are the fitting results using the Jonscher's power law.

lines are obtained from the fit of the Jonscher's power law of the ac conductivity, which in disordered system can be written as [13,14].

$$\sigma(\omega) = \sigma_{dc}\left[1 + (\frac{\omega}{\omega_h})^s\right], \tag{6}$$

where σ_{dc} is the dc conductivity, ω_h is the hopping frequency of the charge carriers, and s is a frequency exponent parameter in the range $0 \leq s \leq 1$, characterizing the deviation from Debye behavior and measuring the inter-ionic-environmental coupling strength [15]. For the $Bi_4Ti_3O_{12}$ glass in this study, s varies from 0.6 to 0.76 at several temperatures, and these values indicate that the system is in a state far away from a Debye-type state (s = 1). It is seen in the figure that the dc conductivity ($\sigma(\omega)$ for $\omega \rightarrow 0$ is obtained from the limiting value of the conductivity plateau region at low frequency) increases and that the hopping frequency ω_h, which is defined to satisfy the relationship of $\sigma(\omega_h) = 2\sigma_{dc}$, shifts to higher frequency with increasing temperature. It should be noticed that the simple power law is applicable to $Bi_4Ti_3O_{12}$ glass for demonstrating the conductivity and the relaxation mechanisms.

Figure 6 is an Arrhenius plot with the symbols obtained from the fit of the Jonscher's power law, Eq. (6). The straight lines in the figure enable us to obtain the conductivity activation energies E_{dc} = 1.07 eV and E_{ac} = 1.02 eV, which are very close to the values E_{dc} = 1.07 eV and E_{ac} = 1.01 eV from the impedance analysis. The similarities of the ac and the dc activation energies calculated from the complex impedance Cole-Cole formalism and from the universal power law imply that the activation energy is an appropriate parameter for describing the electrical relaxation and conduction mechanisms.

Figure 7 shows the conductivity master curves for several temperatures in the glass region. For this master curve, the non-dimensional ac conductivity can be expressed as a function with a non-dimensional frequency in the following scaling form [16]:

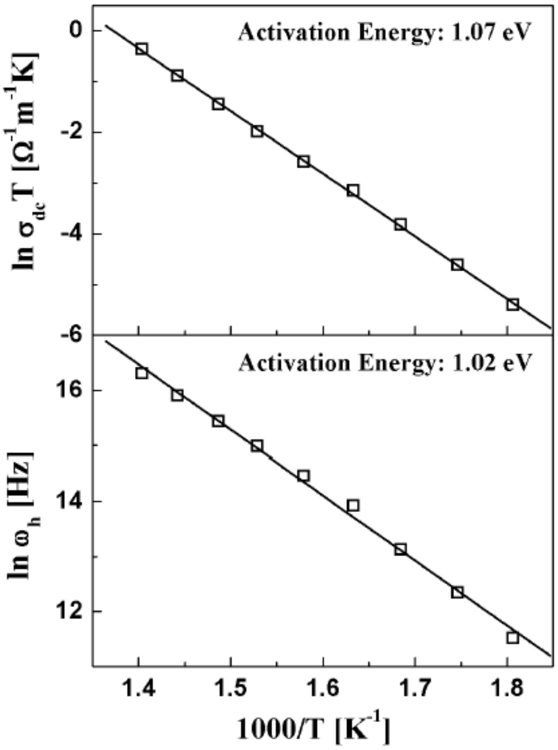

Fig. 6. Arrhenius plot to obtain the dc and the ac activation energies of the conductivity for $Bi_4Ti_3O_{12}$ glass by using the Jonscher's power law.

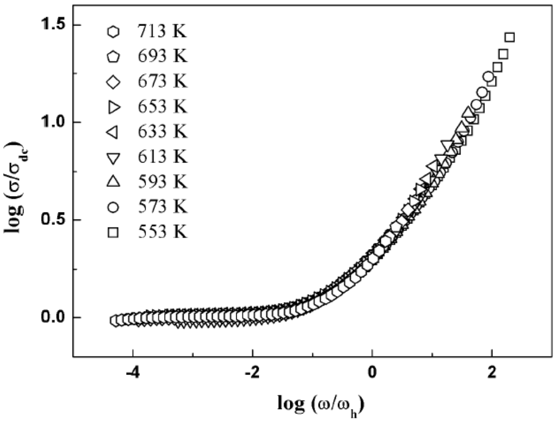

Fig. 7. Frequency-dependent conductivity master curves at several temperatures for $Bi_4Ti_3O_{12}$ glass.

$$\frac{\sigma(\omega)}{\sigma_{dc}} = F\left(\frac{\omega}{\omega_h}\right). \tag{7}$$

As one can be seen in Fig. 7, the individual curves, by introducing a scaling factor, overlap on a single master curve. This indicates that although the electrical conduction increases due to the increased hopping rate of charge carriers with increasing temperature, the electrical conductivity mechanism is independent of temperature: namely, the production of a master curve implies the existence of a universal ionic relaxation process in this glass system.

IV. CONCLUSION

The electrical conduction and dielectric relaxation of $Bi_4Ti_3O_{12}$ glass have been investigated. The real and the imaginary parts of the dielectric constant increase due to the increased hopping rate of ionic charge carriers with increasing temperature in the glass region. The frequency-dependent dielectric constants ε' and ε'' exhibit low-frequency dispersion.

The values of the exponent parameters α and s, obtained from a complex impedance and power law analysis, imply that the dielectric relaxation of $Bi_4Ti_3O_{12}$ glass has a non-Debye behavior, which is thought to originate from ionic conduction of hopping among random free-energy barriers with a broad distribution of relaxation times. We have obtained ac and dc activation energies of electrical conduction by using two different models, the complex impedance formula and the universal power law, and found those values to be close to each other for both models, which indicates that the activation energy is an appropriate parameter for explaining the dielectric relaxation and conduction mechanisms. In the frequency-dependent conductivity at several temperatures, the individual curves overlap on a single master curve, indicating the existence of a universal ionic relaxation process in this glass system.

ACKNOWLEDGMENTS

This work was supported for two years by Pusan National University Research Grant.

REFERENCES

[1] E. C. Subbarao, Phys. Rev. **122**, 804 (1961).

[2] H. Irie, M. Miyayama and T. Kudo, J. Appl. Phys. **90**, 4089 (2001).

[3] Y. Noguchi and M. Miyayama, Appl. Phys. Lett. **78**, 1903 (2001).

[4] T. Kobayashi, Y. Noguchi and M. Miyayama, Appl. Phys. Lett. **86**, 012907 (2005).

[5] T. Jardiel, A. C. Caballero and M. Villegas, J. Eur. Ceram. Soc. **27**, 4115 (2007).

[6] M. Takashige, S. Hamazaki , R. Yoshida, M. Kokubun, F. Shimizu, T. Yamaguchi, M. S. Jang and S. Kojima, Jpn. J. Appl. Phys. **40**, 5816 (2001).

[7] S. Kojima, A. Hushur, F. Jiang, S. Hamazaki, M. Takashige, M. S. Jang and S. Shimada, J. Non-cryst. Solids **293**, 250 (2001).

[8] Y. Yoneda, J. Mizuki, S. Kohahra, S. Hamazaki and M. Takashige, J. Appl. Phys. **99**, 074108 (2006).

[9] A. K. Jonscher, *Universal Relaxation Law* (Chelsea Dielectrics Press, London, 1996).

[10] J. S. Kim, B. C. Choi, B. K. Moon, B. E. Jun, S. B. Cho and J. H. Jeong, J. Korean Phys. Soc. **53**, 1617 (2008).

[11] A. K. Jonscher, *Dielectric Relaxation in Solids* (Chelsea Dielectrics Press, London, 1983).

[12] Y. H. Rim, B. S. Lee, H. W. Choi, J. H. Cho and Y. S. Yang, J. Phys. Chem. B **110**, 8094 (2006).

[13] C. H. Song, M. Kim, H. W. Choi, H. J. Kim and Y. S. Yang, J. Korean Phys. Soc. **51**, S71 (2007).

[14] C. H. Song, H. W. Choi, M. Kim, G. Y. Jin and Y. S. Yang, J. Korean Phys. Soc. **51**, 674 (2007).

[15] K. L. Ngai, R. W. Rendell and H. Jain, Phys. Rev. B **51**, 2770 (1995).

[16] B. Roling, Solid State Ionics **105**, 185 (1998).